# Improved Error Localization in DSL Systems Based on the Common Mode

Oana Graur and Werner Henkel
Jacobs University Bremen, Transmission Systems Group (TrSys)
E-mail {o.graur, w.henkel}@jacobs-university.de

***Abstract*—We propose a scheme to improve system performance in Discrete MultiTone systems, which combines the joint differential and common mode processing at the receiver side with erasure marking. This is achieved by using the strong correlation between differential and common mode in the case of a few strong interferers to obtain an estimate of the impulse noise or RFI, which is used for error localization before decoding. When side information is available, a Reed Solomon (RS) decoder is able to correct twice as many erasures than errors.**

***Index Terms*—erasure, common-mode, impulse noise, DSL system, Reed Solomon code**

## I. Introduction

The conventional approach of using differential mode signaling (DM) to convey information over copper cables is extended to incorporate the common-mode (CM) signal. Since there is a high correlation between CM and DM, the CM signal can be used as side information at the receiver side in order to estimate erasure positions introduced by disturbances such as impulse noise, radio frequency interference (RFI), and crosstalk. Although the current paper focuses on erasure marking when impulse noise is present in the system, the proposed scheme is applicable to any disturbance type which shows a high correlation between CM and DM. Before the proposed method is described, an introduction to DM (differential mode) and CM (common mode) signals may be necessary. Differential mode signaling has been successfully used as the transmission scheme in wireline communications due to its resilience to electromagnetic interference. Differential Mode (DM) signals are complementary signals sent on two separate wires. The receiver measures the voltage difference between the two balanced lines. This fact is illustrated in Fig. 1 a). Assuming $180^\circ$ out of phase square waves of $1V$ sent on the two lines, the receiver would measure a 2 V peak-to-peak square wave. In the case of Common-Mode signaling, which is defined as the arithmetic mean of the signals received on the two wires, measured with respect to ground, the measured output would be 0 V. When interference is introduced additively to the system, Fig. 1 b) illustrates the CM and DM outputs. This would be the ideal case when external interference couples identically into both wires. In practical situations, this is not entirely valid and although differential signaling on balanced lines is, by design, less prone to ingress than other signaling methods, the residual interference that makes it to the receiver side can be critical enough to result in transmission errors. For a mathematical description of signals received in DM and CM in a multi-pair DSL system, which takes into account an arbitrary number of near- and far-end crosstalk disturbances, the reader is referred to [1]. Previous work in the area of joint DM-CM processing can be found in [2]–[4].

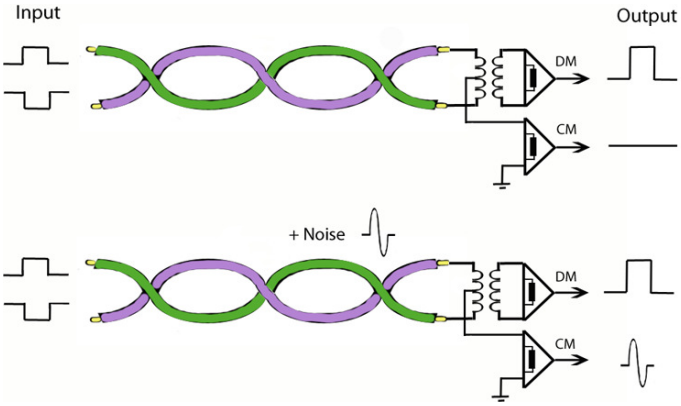


Fig. 1. DM vs. CM signaling. Here, square pulses have been used for illustrative purposes, which is not the case in practical situations. The simulation results described in Section V have been obtained by employing an Asymmetric Digital Subscriber Line (ADSL) transmission system as described in [5].

Statistical properties of impulse noise along with some modeling parameters are discussed in Section II. The idea of erasure marking along with a description of conventional RS (Reed-Solomon) codes can be observed in Section III. A description of the erasure marking scheme proposed in this paper can be found in Section IV. In Section V, it is shown through simulation results that the proposed method provides a considerable performance improvement for Discrete MultiTone (DMT) systems in a highly impulsive environment. Concluding remarks are presented in Section VI.

## II. Impulse Noise

Given its non-stationary nature, impulse noise represents a major impairment in wireline systems. It can originate from a variety of sources, such as industrial appliances, electrical discharges, switching events, etc.. Sets of impulses were measured at phone outlets in different locations in Germany, being caused by different sources, e.g., furnace ignition, trains, trams, fluorescent light switching, welding etc. and their normalized histograms of impulse durations are shown in Fig. 2.

The impulse inter-arrival times used for the simulations in

978-1-4577-2053-6/12/$31.00 ©2012 IEEE

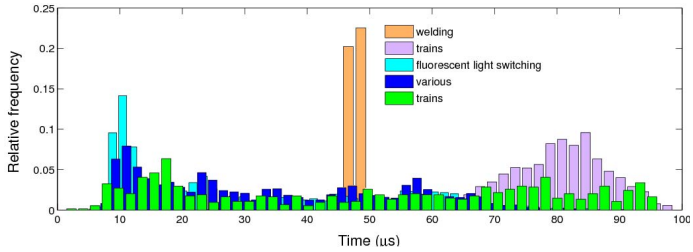


Fig. 2. Normalized histograms of impulse duration. The sets of impulses were measured in different locations in Bremen, Germany, and were caused by various sources, e.g., welding, fluorescent light switching, etc.

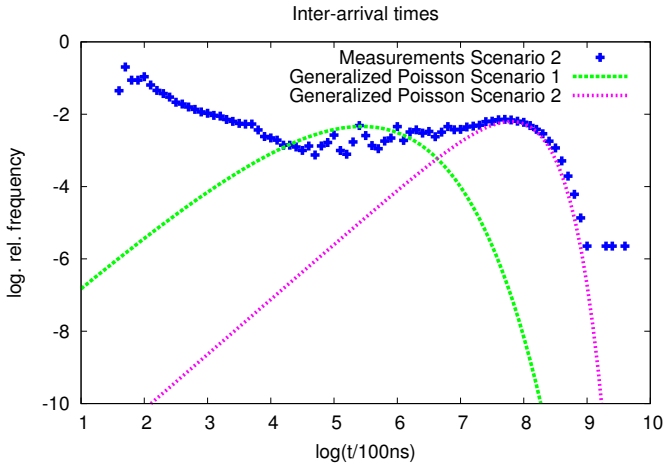


Fig. 3. Logarithmic plots of impulse inter-arrival time approximated by generalized Poisson distributions with parameters in Table I.

Section V obey the generalized Poisson distribution given in (1), with the parameters specified in Table I. An extensive description of the probability density function (PDF) of inter-arrival times, along with other parameters for impulse noise modeling such as amplitude and duration, is found in [6]–[9]. Figure 3 is a logarithmic plot of the distributions in (1).

$$f_d(x) = \frac{10^{a_1}}{\ln(10)} x^{a_4-1} 10^{-\frac{a_4}{\ln(a_2)} a_2^{\log_{10}(x)-a_3}} \qquad (1)$$

The measurement points on the left side of the plot that do not appear to fit the approximation are considered as gaps within the impulses, due to their extremely short duration, and are discarded. For the results in Section V, two different scenarios have been considered, one with an inter-arrival distribution characteristic for an industrial environment, or an old-fashioned central office, with strong impulsive disturbers, and one distribution suitable for a customer premise environment, slightly impulsive. As will be shown in the results section, the gain obtained by employing the proposed scheme becomes highly significant in the case of a highly impulsive environment. The measured impulses used for the simulations presented in Section V had a maximum peak-to-peak voltage of 1 V.

TABLE I
INTER-ARRIVAL DISTRIBUTION PARAMETERS [a]

| Scenario | $a_1$ | $a_2$ | $a_3$ | $a_4$ | x |
|---|---|---|---|---|---|
| #1 | -7.54 | 1.88 | 5.44 | 1.52 | t/100 ns |
| #2 | -12.54 | 5.88 | 7.8 | 1.52 | t/100 ns |

[a] Both scenarios are obtained from sets of measurements taken in Germany. First scenario is at a CO and second scenario is at customer premises. First coefficient is computed such that the area under the curve integrates to 1.

## III. Error and Erasure Coding in DMT Systems

Wireline systems are prone to transmission errors caused by ingress. These errors can occur at random time instances or in isolated finite-length sequences, in the case of impulse noise and RFI, known as bursts.

Many codes can successfully correct errors occuring in AWGN environments but are unsuccessful in the case of error bursts typically caused by impulse noise. More burst errors present in a codeword can cause the decoder to fail retrieving the correct information. Reed-Solomon codes have been chosen for DSL transmission due to their multiple-burst error correction capability and analytical performance computation. Assuming the error locations to not be known in advance, Reed-Solomon codes are able to correct up to $(n-k)/2$ erroneous symbols, where $(n-k)$ represents the number of redundant symbols in a block ($n$: length of codewords, $k$: number of information symbols).

If side information is present at the demodulator and erasure marking is possible, a Reed-Solomon code is able to decode twice as many erasures than errors, or any combination of errors and erasures as long as

$$s + 2(e - v) \leq 2t = n - k \,, \qquad (2)$$

where $s$ is the number of erasures, $e$ is the number of errors, $v$ gives the number of the errors and erasures that overlap and $t$ is the error correcting capability of the code. In the case of a multitone system, the energy of the impulse noise and RFI will be spread among many subchannels. As the interference strength is further increased, a major portion of the DMT block will be affected, unlike the single-carrier case where only a few symbols are affected. To compensate for this drawback, a code such as Reed Solomon is more effective in a multitone system when used in conjuction with interleaving. If the number of erroneous symbols $b$ in a codeword is smaller than the error correcting capability of the code, namely $t$, then the codeword will be successfully decoded, otherwise spreading the error burst to multiple codewords is necessary. Interleaving ensures a higher probability that the number of erroneous symbols in each codeword would be less than $t$. Interleaving will, thus, increase the burst-error correction capability by the interleaving depth as a factor.

## IV. Proposed Scheme

Given the fact that in wireline systems, the CM signal is available on the receiver side with limited extra costs and

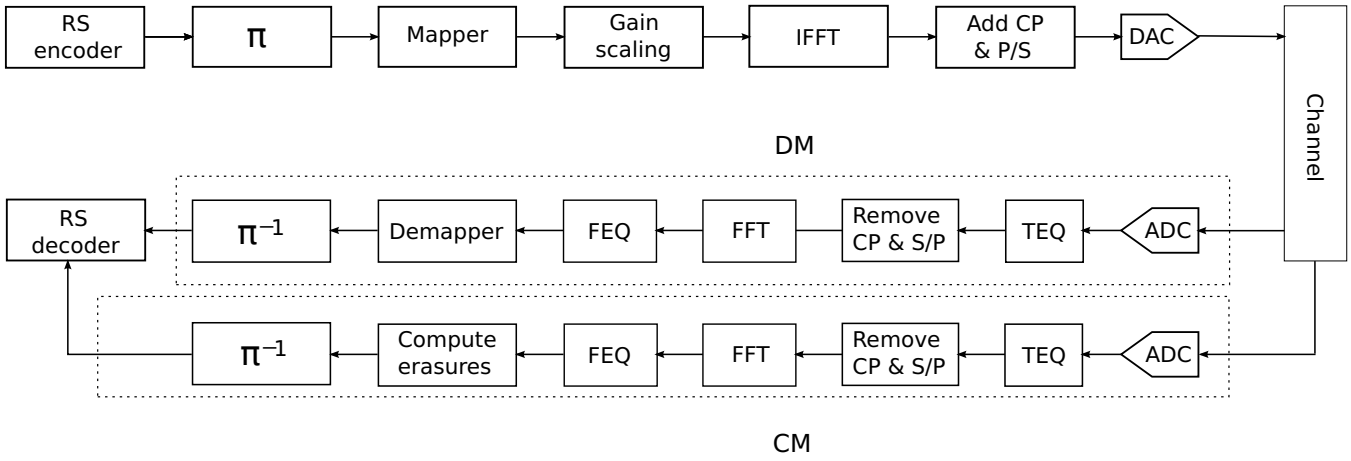


Fig. 4. Proposed system diagram. No changes are necessary at the transmitter side. At the receiver side, joint DM-CM processing is performed.

there is a strong correlation between DM and CM, this can be exploited to flag erasure positions for RS decoding. At the receiver, both the DM signal and the impulse noise estimate signal obtained from CM are processed in parallel. As depicted in Fig. 4, no changes are necessary at the transmitter side. At the receiver, along with the standard differential signal, a common mode measured signal is passed through an ADC converter. The effect of intersymbol interference (ISI) is mitigated by a time domain equalizer (TEQ), assuming an Asymmetric Digital Subscriber Line (ADSL) system, where the need to shorten the channel impulse response is justifiable. After the TEQ, the guard interval is removed and the remaining samples are converted into parallel data streams before the Discrete Fourier Transform (DFT) operation. After the frequency domain equalizer (FEQ), the DM signal is further passed on to the demapper, deinterleaver, and RS decoder, while the estimated impulse originating from the CM measurement is thresholded in order to obtain the positions of the carriers affected by impulse noise. Once the estimated corrupted carrier positions have been determined, the bits allocated to those carriers are marked as erasures and the information is passed on to the RS decoder. For power consumption constraints, the erasure marking scheme proposed should only be active when the common mode signal level exceeds a certain threshold $\lambda$, since this flags the presence of strong interference in the system. The scheme proposed is not limited to the case of impulse noise, but also RFI and narrowband interference, such as that originating from nearby AM stations, or any other source, as long as the number of disturbers is limited to a few. This ensures a high correlation between CM and DM. For this reason, no benefits can be gained in the case when only background noise is present in CM, and the choice of the threshold $\lambda$ should clearly be greater than the background noise level.

### A. Impulse noise estimation

Given an impulse measured in CM, and knowing the transfer function between DM and CM ($H$) beforehand, also known in literature as the Transverse Conversion Transfer Loss (TCTL), an estimate of the DM impulse can be obtained as in (4), where $\hat{I}_{dm}(jw)$ is the DFT domain estimate of the current impulse present in DM and $I_{cm}(jw)$ is the DFT domain counterpart of the current impulse measured in CM. The transfer characteristic between differential and common mode was practically obtained from the average pseudo[1] cross power spectral density of DM ($S_{CM-DM}(jw)$) and the average pseudo power spectral density of CM ($S_{CM-CM}(jw)$), with noise averaged out, as in (3). The channel is assumed to be linear and time invariant, which is a reasonable assumption for wireline systems.

$$H(jw) = \frac{S_{CM-DM}(jw)}{S_{CM-CM}(jw)} \tag{3}$$

$$\hat{I}_{dm}(jw) = I_{cm}(jw)H(jw) \tag{4}$$

### B. Carrier marking

Once the estimate is available, the bits present on the carriers affected by impulse noise are flagged as erasures when the absolute[2] value $|\hat{I}_{dm}(jw)|$ of the impulse noise estimate exceeds a certain level $\tau$. The choice of this threshold is critical, since it determines the number of erasures in a DMT symbol. A larger value of the threshold would yield a smaller number of erasures, while a smaller value would increase the number of erasures. For the carrier marking step, two scenarios have been compared: one which uses a constant threshold $\tau = \eta$ for all carriers, and a second scenario with an carrier-adaptive threshold $\tau[i]$, where $i$ denotes the DMT carrier index.

In the hypothetical case when the actual impulse in DM would be known, with a DFT domain vector given by $I_{dm}(jw)$, a constant threshold $\eta$ would suffice to correctly determine all error positions (in Eq. (2), $e = s = v$). Since $I_{dm}(jw)$ is not available and the estimate $\hat{I}_{dm}(jw)$ is used

[1]Since a non-stationary process has no power spectral density, the term pseudo power spectral density will be used to refer to the symbol duration, considering the cases when impulses are present in that symbol.

[2]Since the thresholding is carried out in frequency domain and the DFT counterpart of the estimated impulse is complex, the absolute value is used.

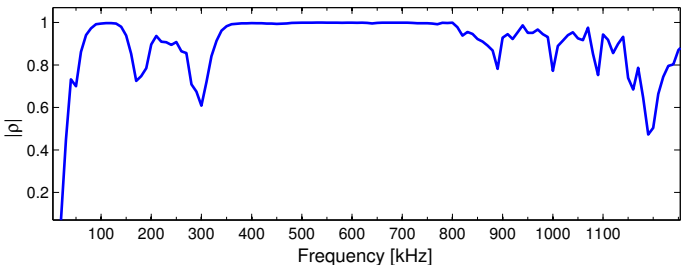


Fig. 5. Frequency dependent correlation coefficient between DM and CM for the ADSL spectral range.

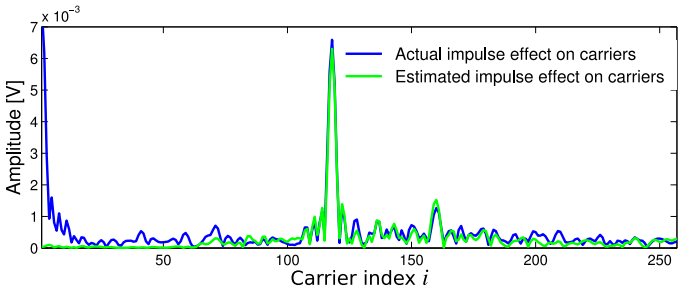


Fig. 6. Carriers corrupted by impulse noise obtained from measurements and estimated impulse noise. For this plot, one measured impulse originating from fluorescent light switching was used.

instead, the constant threshold $\eta$ should be rescaled by the ratio $\frac{E\{|\hat{I}_{dm}|\}}{E\{|I_{dm}|\}}$ as given in (5), where $E$ denotes expectation. Here, $|H|^2$ has been rephrased as $\frac{S_{DM}}{S_{CM}}$, where $S_{DM}$ and $S_{CM}$ are the pseudo power spectral densities of DM and CM, and $N_{DM}$ and $N_{CM}$ are the pseudo power spectral densities of the noise in DM and CM, respectively. The notation $(jw)$ has been omitted, i.e., has been replaced by the carrier index $i$.

$$\tau[i] = \eta \frac{\sqrt{(S_{CM}+N_{CM})\frac{S_{DM}}{S_{CM}}}}{\sqrt{S_{DM}+N_{DM}}} = \eta \sqrt{\frac{\frac{S_{DM}[i]}{S_{CM}[i]}}{\frac{S_{DM}[i]+N_{DM}[i]}{S_{CM}[i]+N_{CM}[i]}}} \quad (5)$$

A high level of uncorrelated noise in CM ($N_{CM}$) will increase the threshold function $\tau[i]$, meaning that the estimate of the impulse obtained by employing the CM-measured signal will have a higher inaccuracy, and for this reason the value of the threshold should be raised, leading to a reduced number of erasures.

The DMT carriers affected by impulse noise and estimated impulse noise are shown in Fig. 6. It can be observed that for middle-range carriers, a more accurate estimation is obtained. This is explained by the fact that there is a higher correlation between CM and DM for that range of frequencies, as depicted in Fig. 5. For a frequency-dependent correlation coefficient, above the ADSL spectral range, the reader is referred to [1].

## V. Simulation Results

For the simulation results depicted in the current section, an ADSL DMT system was implemented, with the parameters summarized in Table II. Figure 7 presents the case of the highly impulsive case, when two different methods for estimating the carrier threshold $\tau$ are used. The optimum contant threshold has been obtained through Monte-Carlo simulations, for every loop length simulated. Both curves are compared with the case when impulse noise is present in the system but the proposed erasure marking scheme is not used, and the case when only AWGN is present and erasure marking is, of course, not activated either. As expected, the adaptive threshold from (5) performs better than a constant threshold throughout the carriers. For the slighly impulsive case, presented in Fig. 8 both thresholding methods yield similar results. The two scenarios under analysis show different gains when the proposed erasure marking scheme is employed. While in the scenario where the transmission is not subject to severe impulsive degradation, the gain of using the proposed scheme is insignificant, in the case of a heavily impulsive environment, a gain of approximately 420 m is observed for a required DSL BER of $10^{-7}$.

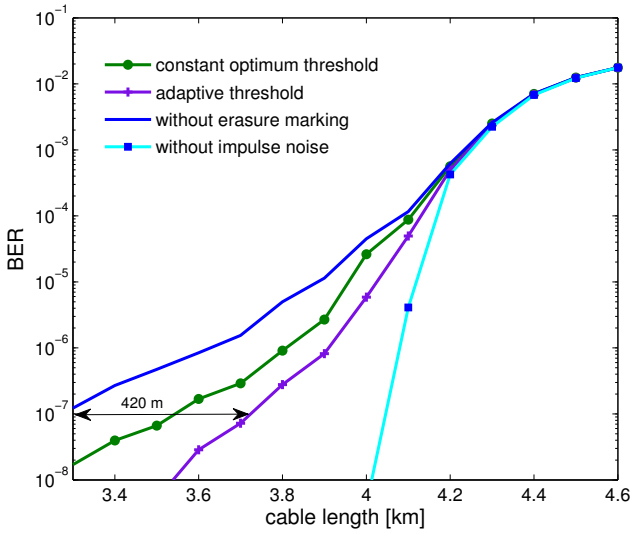


Fig. 7. Scenario #1: BER after RS decoding for the highly impulsive environment. The proposed erasure marking scheme has a significant gain when presented with a strongly impulsive case.

For the simulations described in Section V, perfect echo cancellation is assumed to be employed in order to distinguish between the upstream and downstream signals.

Since the CM signal processing is done in parallel with the DM, latency is not a serious issue to consider. The dominant component responsible for the increased cost and power consumption in the receiver is the extra ADC converter necessary for the CM processing. Also, a second DFT operation is required. Nevertheless, the extra costs introduced by the DM-CM joint processing at the receiver side become justifiable in the case of strong interferers disrupting the transmission system.

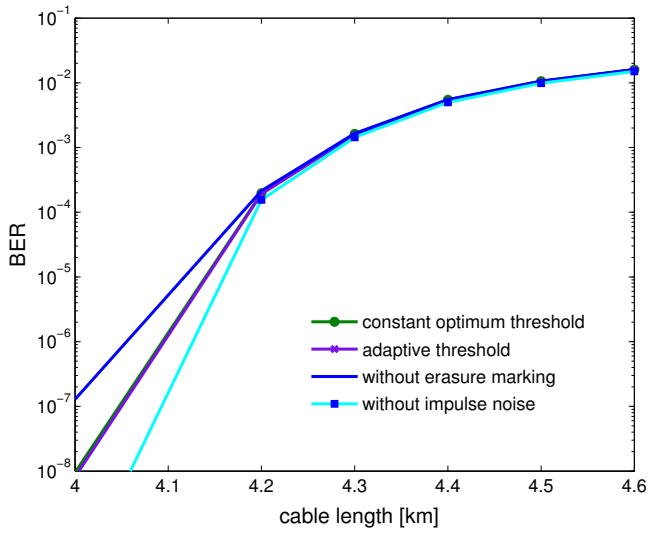


Fig. 8. Scenario #2: BER after RS decoding for the slightly impulsive environment. As expected, when the main interference source is AWGN and no other stronger interferers are present, the improvement obtained by employing the erasure scheme is not very significant.

TABLE II
ADSL SIMULATION PARAMETERS

| **Reed Solomon (RS) Code Parameters** | |
|---|---|
| Interleaver depth $d$ | 32 |
| DMT symbols in RS codeword $s$ | 2 |
| Information symbols $k$ in RS codeword | 134 |
| Error correcting capability $t$ | 6 |
| RS symbol size | 8 bits |
| **DMT Downstream [a] Parameters** | |
| AWGN | -120 dBm/Hz |
| Number of carriers | 254 |
| Downstream net rate | 2.048 Mbit/s |
| Reserved carriers | 0–5, 96 |
| Carrier spacing | 4.3125 kHz |
| Cable diameter | 4 mm |
| Transmit power | 20 dBm |
| Sampling rate | 2.208 MHz |
| Loop range | 2.6 - 4.6 km |
| Cyclic prefix | 32 samples |
| Number of NEXT disturbers [b] | 4 AslMx |

[a] Simulations were performed for downstream only.
[b] FEXT effect is considered negligible for cable loops longer than 2 km.

## VI. SUMMARY AND CONCLUSION

In the previous section, simulation results have shown that in the case of DMT (Discrete MultiTone) transmissions, when the correlation between CM and DM is exploited in order to provide erasure positions for a RS decoder with interleaving, a gain of $420$ m for a $0.4$ mm diameter cable is attained for a required BER of $10^{-7}$. An almost standard-compliant ADSL system has been implemented in order to evaluate the performance of the proposed scheme. In practical situations, the gain obtained in the case of highly impulsive scenarios compensates for the increased hardware complexity at the receiver side. The proposed erasure scheme is not limited to impulse noise, it can be extended to RFI and crosstalk as long as there is a small number of disturbers and there is a high correlation between the interference present in CM and DM.

## ACKNOWLEDGMENT

This work is supported by the German National Science Foundation (Deutsche Forschungsgemeinschaft – DFG).

## REFERENCES

[1] O. Graur and W. Henkel, "Impulse-Noise Cancellation Utilizing the Common-Mode Signal to Improve the Bit-Error Ratio in DSL Systems," in *15th International OFDM-Workshop 2010*, Hamburg, Germany, September 2010.

[2] T. Magesacher, P. Ödling, and P. O. Börjesson, "Analysis of Adaptive Interference Cancellation Using Common-Mode Information in Wireline Communications," *EURASIP J. Adv. Signal Process*, vol. 2007, pp. 9–9, June 2007.

[3] T. Magesacher, P. Ödling, P. O. Börjesson, and T. Nordström, "Exploiting the Common-Mode Signal in xDSL," *European Signal Processing Conference*, 2004.

[4] T. Magesacher, P. Ödling, and P. O. Börjesson, "Adaptive Interference Cancellation using Common-Mode Information in DSL," in *Proc. European Signal Processing Conf. EUSIPCO 2005*, Antalya, Turkey, September 2005.

[5] "Test Procedures for Digital Subscriber Line (DSL) Transceivers," International Telecommunication Union, Draft ITU-T Recommendation G.996.1, February 2001.

[6] W. Henkel, T. Kessler, H. Chung, and H. Y. Chung, "A Wide-Band Impulse-Noise Survey On Subscriber Lines And Inter-Office Trunks - Modeling And Simulation," in *Lines and Inter-Office Trunks - Modeling and Simulation, Globecom/CTMC '95*, 1995, pp. 13–17.

[7] I. Mann, S. McLaughlin, W. Henkel, R. Kirkby, and T. Kessler, "Impulse Generation with Appropriate Amplitude, Length, Inter-arrival, and Spectral Characteristics," *IEEE Journal on Selected Areas in Communications*, vol. 20, no. 5, pp. 901–912, June 2002.

[8] W. Henkel, T. Kessler, and H. Chung, "Coded 64-CAP ADSL in an Impulse-Noise Environment - Modeling of Impulse Noise and First Simulation Results," *IEEE Journal on Selected Areas in Communications*, vol. 13, no. 9, pp. 1611–1621, December 1995.

[9] W. Henkel and T. Kessler, "A Wideband Impulsive Noise Survey in the German Telephone Network: Statistical Description and Modeling," *AEÜ*, vol. 48, no. 6, pp. 277–288, Nov.-Dec. 1994.